

 **Los Alamos**
NATIONAL LABORATORY
— EST. 1943 —

Delivering science and technology
to protect our nation
and promote world stability



Subcritical Copper-Reflected α -phase Plutonium (SCR α P) Measurements and Simulations

J. Hutchinson, R. Bahran, T. Cutler, W. Monange*, J. Arthur,
M. Smith-Nelson, E. Dumonteil*

Los Alamos National Laboratory

**Institut de Radioprotection et de Sûreté Nucléaire (IRSN)*



NCSP TPR
March 2017



Overview

- Introduction
- Experiment Design
- Experiment Overview
- **Preliminary** Results
- Future work

Introduction

Design/Conduct/Analyze Subcritical Validation Experiments

○ Nuclear Data and Transport Codes

- Fill integral experiment database deficiencies

+

- Find differential nuclear data library deficiencies

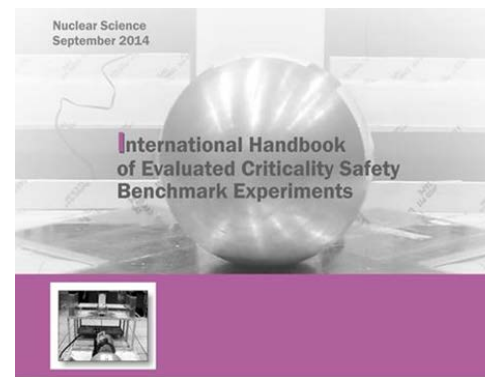
For different....

- Energy Ranges (Thermal, Intermediate, Fast)
- Multiplication Ranges (Low, Medium, High)
- Materials (Fissile, Moderator, Reflector)
- Neutron Reactions

○ Uncertainty Quantification

Recent Advances in Subcritical Experiments

- We have come a long way since the first subcritical measurements at CP-1 in 1942.
- Many organizations (LANL, LLNL, SNL, IAEA, IRSN, CEA, universities, and others) have pursued subcritical experiments and/or simulations in recent years.
- The BeRP ball reflected by nickel benchmark evaluation was published in the 2014 edition of the ICSBEP handbook.
- **This benchmark was the first:**
 - Published benchmark evaluation of measurements performed at DAF.
 - Benchmark evaluation using new MCNP capabilities for subcritical systems (the MCNP list-mode patch and MCNP6 list-mode capabilities).
 - Benchmark using the Feynman Variance-to-Mean method.
 - LANL-led subcritical experiment in the ICSBEP handbook.
- **This benchmark was the culmination of several years of subcritical experiment research.**
- **BeRP-tungsten published in 2016 edition of ICSBEP handbook.**



Experiment Design (CED-1 and CED-2)

Subcritical Copper-Reflected α -phase Plutonium (SCR α P) Integral Experiment

- **SCR α P Preliminary Design (w/ MCNP[®]6)**
 - BeRP (Beryllium-Reflected Plutonium).
 - 4.5-kg WG α -phase stainless-steel clad plutonium sphere.
 - High-purity nested copper shells
 - C101 Cu alloy (99.99 wt.% Cu).



Subcritical Copper-Reflected α -phase Plutonium (SCR α P) Integral Experiment

- **SCR α P Preliminary Design (w/ MCNP[®]6)**
 - High-density interleaved polyethylene shells
- **Wide range of achievable subcritical multiplication values will help:**
 - Identify deficiencies and quantify uncertainties in nuclear data
 - Validate computational methods related to neutron multiplication inference.



There are two purposes for the configurations with polyethylene:

- They allow for higher multiplication factor than with copper alone
- They allow for a different neutron spectra (and resulting sensitivity) for the same multiplication factor.

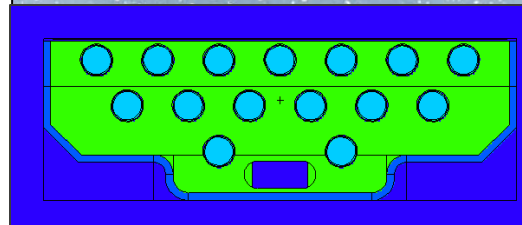
Subcritical Copper-Reflected α -phase Plutonium (SCR α P) Integral Experiment

- MC-15 (Multiplicity Counter 15) was used to estimate three benchmark parameters:
 - Detector singles count rate (R_1) i.e. the count rate in the detector system
 - Doubles count rate (R_2) i.e. the rate in the detector system in which two neutrons from the same fission chain are detected
 - Leakage multiplication (M_L) i.e. the number of neutrons escaping a system per starter neutron.



Records list-mode data (a time list of every recorded neutron event to a resolution of 128 nsec).

Photograph and MCNP® model of the MC-15 detector system.



15 He-3 tubes inside polyethylene.

Subcritical Copper-Reflected α -phase Plutonium (SCR α P) Integral Experiment

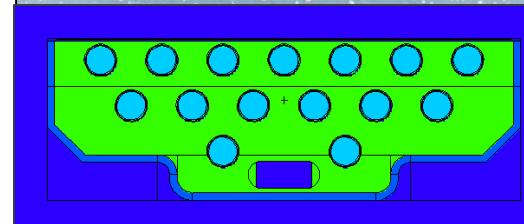


For the SCR α P experiment, two MC-15 systems were present and collected data in the same time list.



Records list-mode data (a time list of every recorded neutron event to a resolution of 128 nsec).

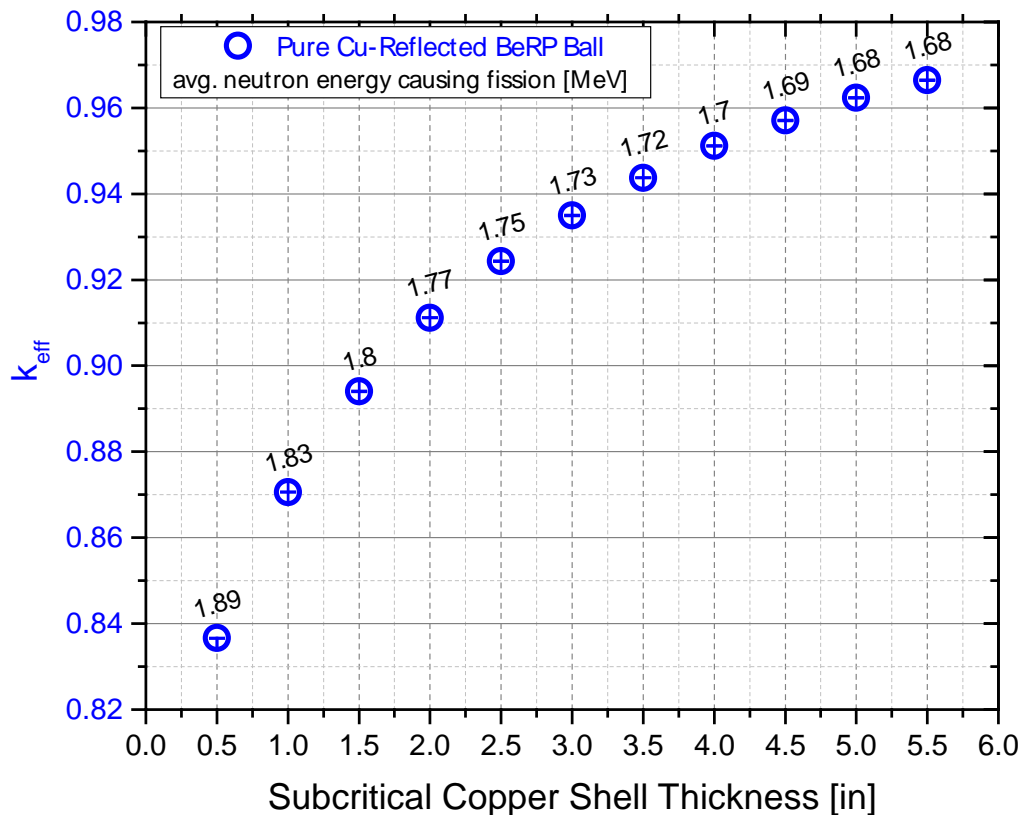
Photograph and MCNP® model of the MC-15 detector system.



15 He-3 tubes inside polyethylene.

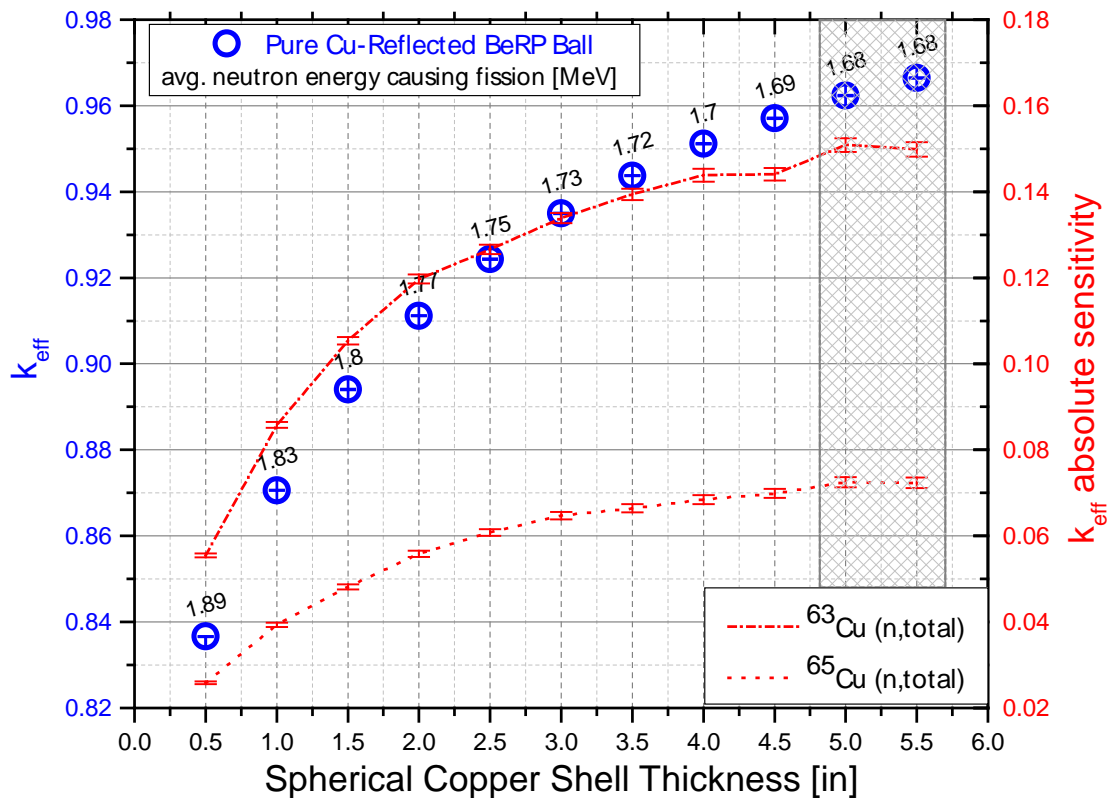
Sensitivity Results with MCNP[®]6

- **Cu-only base configurations shown.**
- **Decided to only measure configurations up to 4.0" thickness of total Cu:**
 - Cu total neutron cross section sensitivity (and average neutron energy causing fission) level out at the 5"-thick mark.
 - Beyond 4.0" there are additional issues (weight, cost, criticality safety).

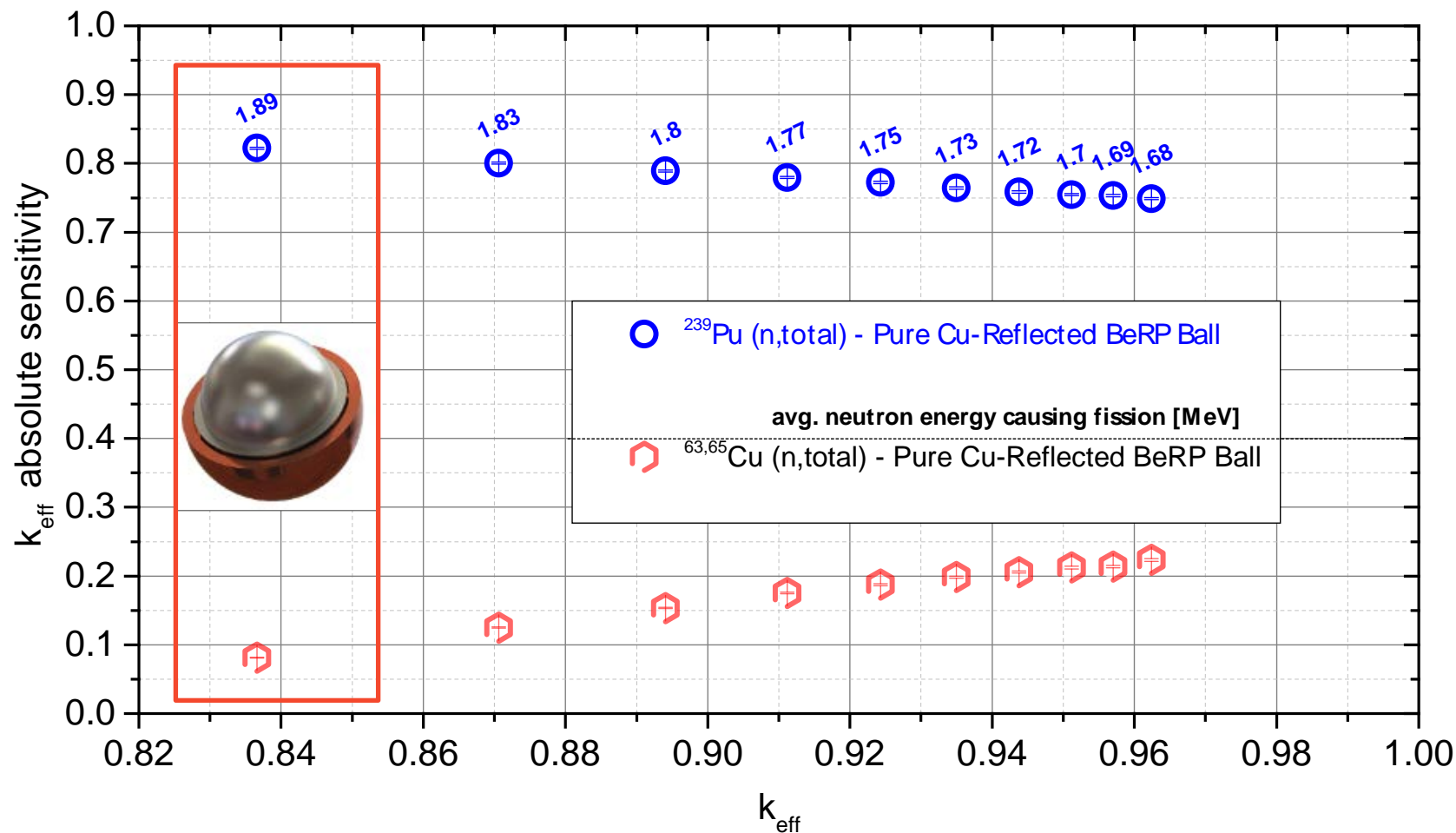


Sensitivity Results with MCNP[®]6

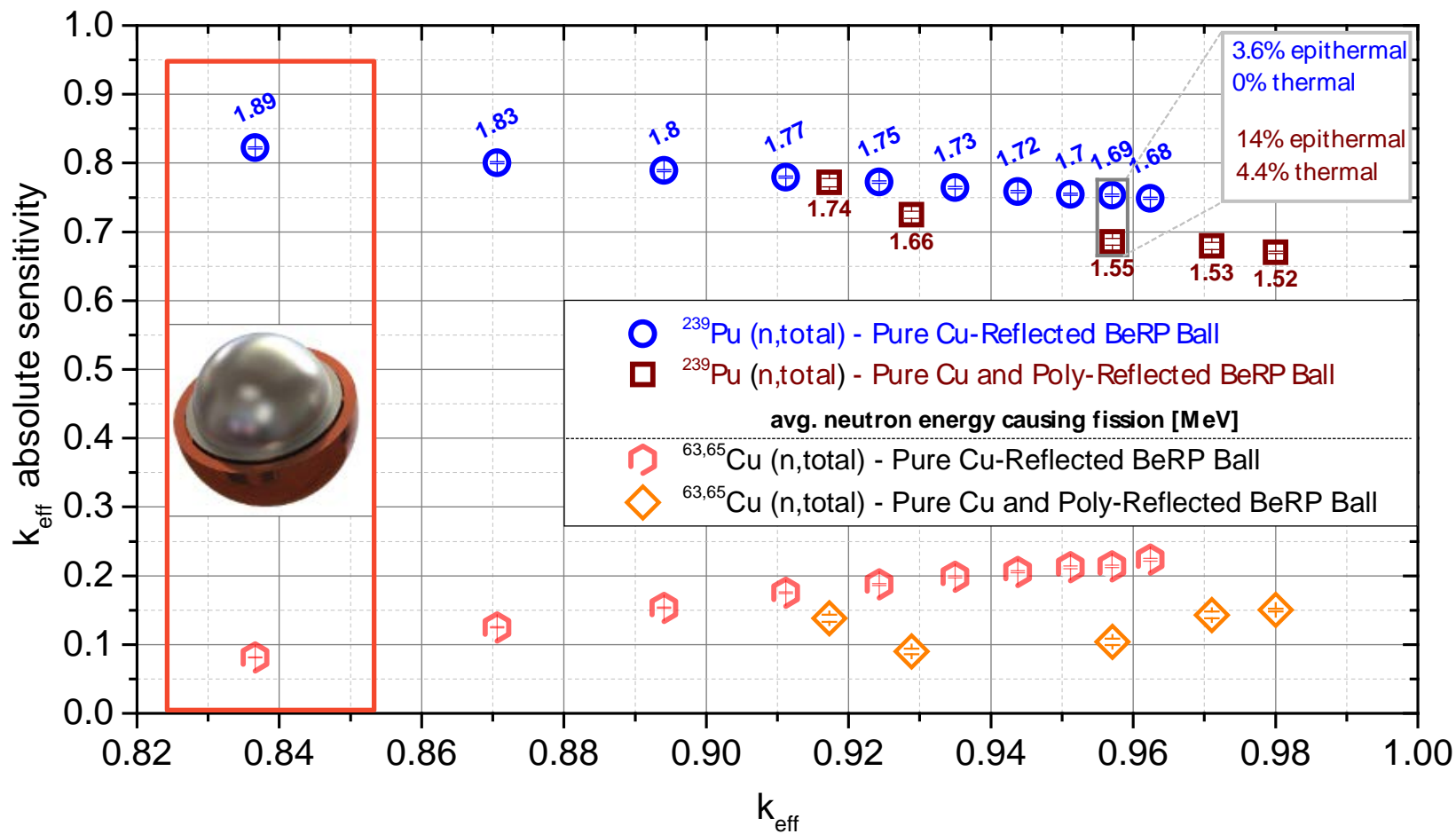
- **Cu-only base configurations shown.**
- **Decided to only measure configurations up to 4.0" thickness of total Cu:**
 - Cu total neutron cross section sensitivity (and average neutron energy causing fission) level out at the 5"-thick mark.
 - Beyond 4.0" there are additional issues (weight, cost, criticality safety).



Interleaving Poly Provides Additional Configurations

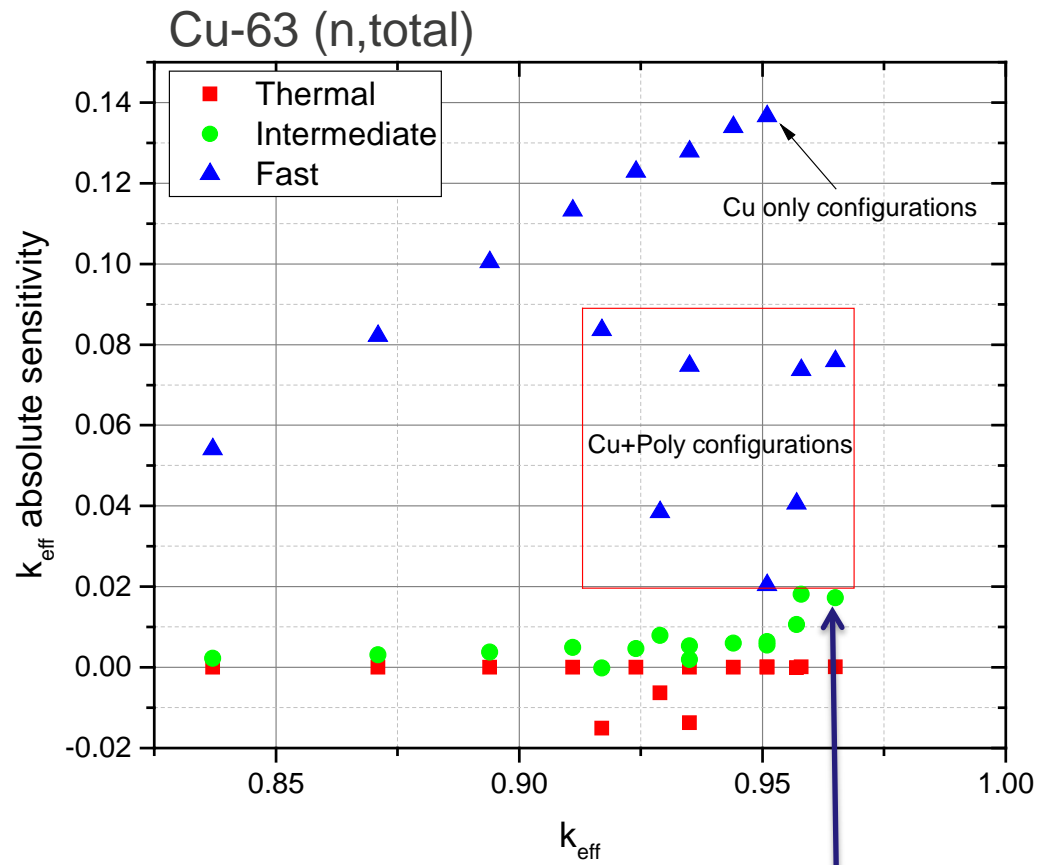


Interleaving Poly Provides Additional Configurations



Sensitivity Results with MCNP[®]6

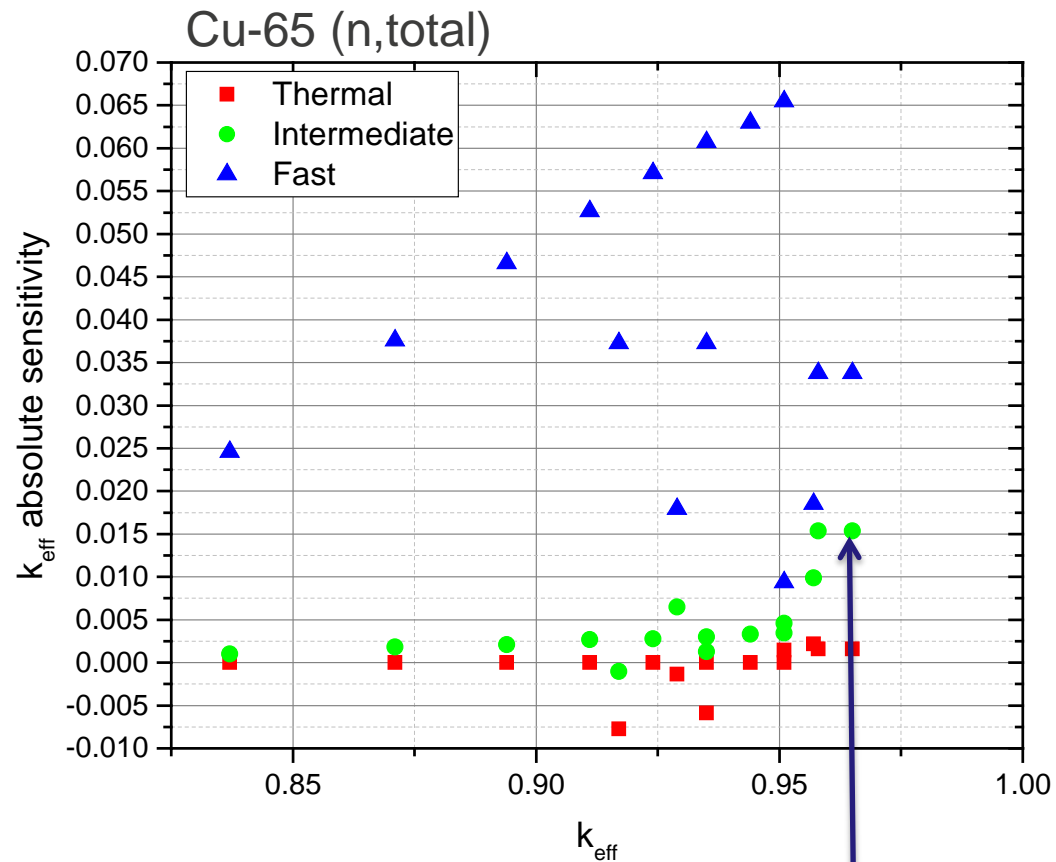
- These results were compared to critical configurations in the ICSBEP handbook.
 - Note that there are a limited number of copper-reflected critical experiments (8 series with U fuel and 2 series with Pu fuel).
- **Total Cu-63 (all energies):**
 - For SCRaP experiment, the maximum sensitivity (0.143) was **greater than the two Pu series** (0.126 max) but **less than for some of the U series** (0.200 max).
- **Total Cu-63 (intermediate energy regime):**
 - For SCRaP experiment, the maximum sensitivity for the 16 configurations (0.018) is **greater than the two Pu experimental series by nearly an order of magnitude** (0.002), but similarly **less than that for some of the U experimental series** (0.051).



Configurations with HDPE have increased sensitivity in the intermediate energy range.

Sensitivity Results with MCNP[®]6

- These results were compared to critical configurations in the ICSBEP handbook.
 - Note that there are a limited number of copper-reflected critical experiments (8 series with U fuel and 2 series with Pu fuel).
- **Cu-65 sensitivity results yielded same conclusions as Cu-63.**



Configurations with HDPE have increased sensitivity in the intermediate energy range.

Uncertainty estimates

- Experimental uncertainties for 4 experimental parameters were calculated.
- Used criticality eigenvalue calculations for these estimates as described in a previous work [J. HUTCHINSON, T. CUTLER “Use of Criticality Eigenvalue Simulations for Subcritical Benchmark Evaluations” Transactions of the ANS Winter Meeting, Las Vegas NV (2016)].

Many lessons-learned from the previous Ni and W benchmarks were used to minimize experimental uncertainties.

Estimate of experimental uncertainties for Configuration 15 (0.5 inch-thick HDPE surrounded by 3.5 inch-thick copper).

Parameter	Experimental Uncertainty	Uncertainty
M_L	Pu radius \pm 2 mils	0.18
	Pu isotopics \pm 0.5%	0.19
	Cu thickness \pm 0.3 cm	0.03
	Cu mass \pm 0.5%	0.00006
R_1	Pu radius \pm 2 mils	1024
	Pu isotopics \pm 0.5%	1045
	Cu thickness \pm 0.3 cm	141
	Cu mass \pm 0.5%	0.34
R_2	Pu radius \pm 2 mils	37450
	Pu isotopics \pm 0.5%	41336
	Cu thickness \pm 0.3 cm	5252
	Cu mass \pm 0.5%	13.1

Cu mass was expected to be a minor uncertainty, which the table confirms.

Experiment Overview (CED-3B)

Experiment configurations

- **17 total configurations:**
 - 1 Bare
 - 8 Cu-only configurations
 - 7 Cu+HDPE configurations
 - 1 HDPE-only configuration
- **In order to determine the detector efficiency, Cf-252 source replacement measurements were performed.**
 - The source strength of the Cf-252 source at the time of the measurements was $7.59e5$ fissions/sec +/- 1.0%.



Configu- ration #	Layer number (each layer is 0.5 inches thick)							
	1	2	3	4	5	6	7	8
0								
1	Orange							
2	Orange	Orange						
3	Orange	Orange	Orange					
4	Orange	Orange	Orange	Orange				
5	Orange	Orange	Grey	Grey	Grey	Grey		
6	Orange	Orange	Orange	Orange	Orange			
7	Grey	Orange	Grey	Orange	Grey	Orange	Grey	Orange
8	Orange	Grey	Orange	Grey	Orange	Grey	Orange	Grey
9	Orange	Orange	Orange	Orange	Orange	Orange		
10	Orange	Orange	Orange	Orange	Orange	Orange	Orange	
11	Orange	Orange	Orange	Orange	Orange	Orange	Orange	Orange
12	Grey	Grey	Grey	Orange	Orange	Orange	Orange	
13	Grey	Orange	Orange	Orange	Orange	Orange	Orange	
14	Grey	Orange	Orange	Orange	Orange	Orange	Orange	
15	Grey	Orange	Orange	Orange	Orange	Orange	Orange	Orange
16	Grey	Grey	Grey	Grey	Grey	Grey	Grey	Grey

Experiment configurations

- **17 total configurations:**
 - 1 Bare
 - 8 Cu-only configurations
 - 8 Cu+HDPE configurations
- **In order to determine the detector efficiency, Cf-252 source replacement measurements were performed.**
 - The source strength of the Cf-252 source at the time of the measurements was $7.59e5$ fissions/sec +/- 1.0%.



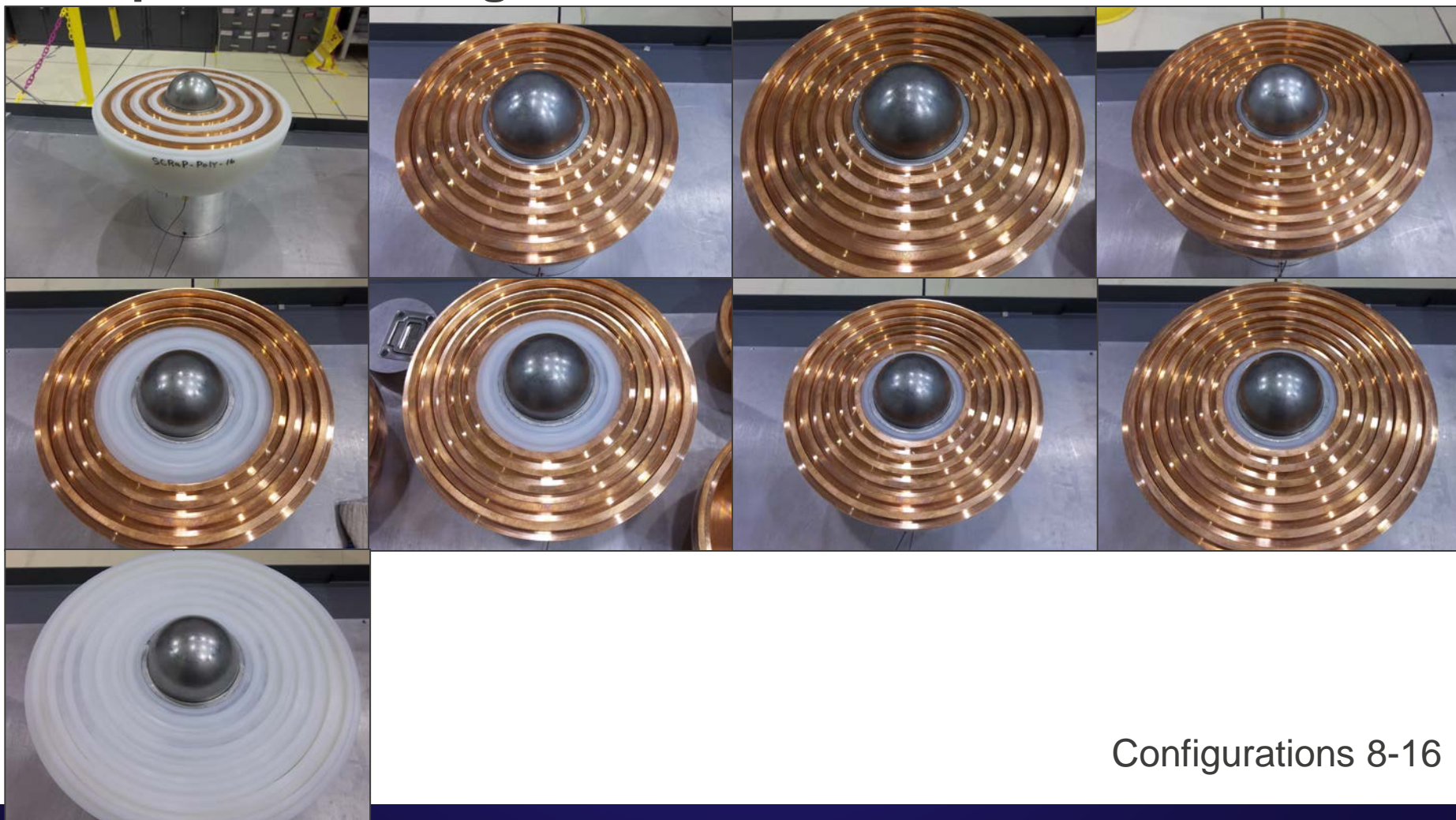
Thickness (inches)			Simulated k_{eff}	
HDPE	Cu	HDPE+Cu	LANL	IRSN
0.0	0.0	0.0	0.774	0.777
0.0	0.5	0.5	0.837	0.829
0.0	1.0	1.0	0.871	0.862
0.0	1.5	1.5	0.894	0.884
0.0	2.0	2.0	0.911	0.900
2.0	1.0	3.0	0.917	0.907
0.0	2.5	2.5	0.924	0.914
2.0	2.0	4.0	0.929	0.921
2.0	2.0	4.0	0.935	0.919
0.0	3.0	3.0	0.935	0.923
0.0	3.5	3.5	0.944	0.933
0.0	4.0	4.0	0.951	0.939
1.5	2.0	3.5	0.951	0.939
1.0	2.5	3.5	0.957	0.943
0.5	3.0	3.5	0.958	0.942
0.5	3.5	4.0	0.965	0.948
4.0	0.0	4.0	-	-

Experiment configurations



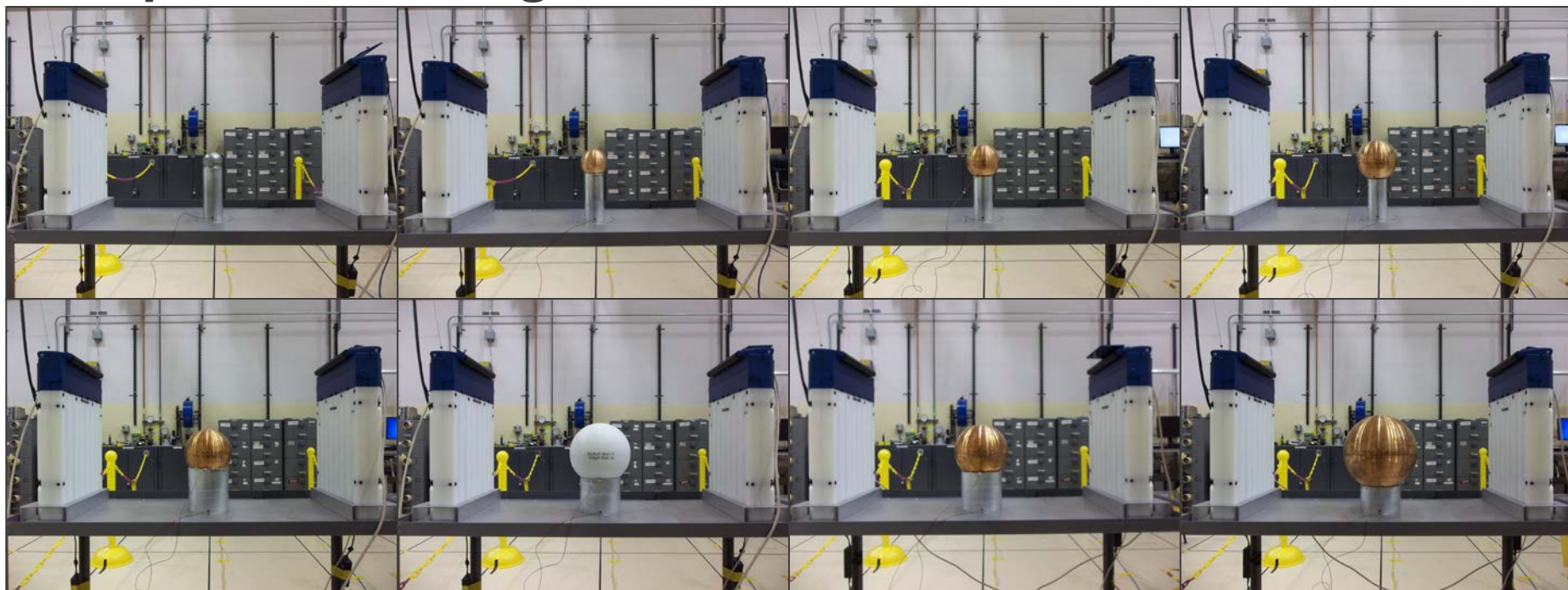
Configurations 0-7

Experiment configurations



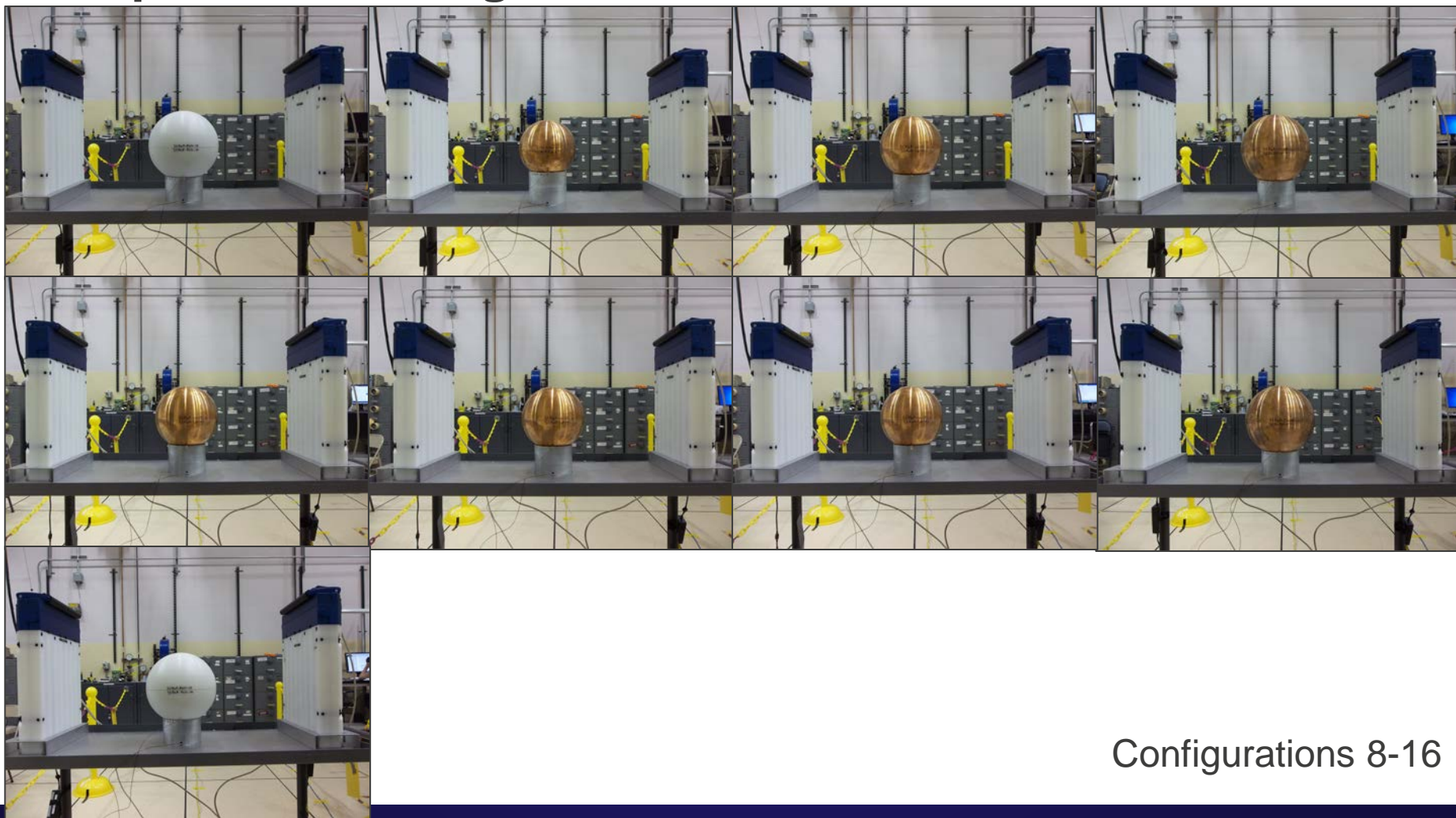
Configurations 8-16

Experiment configurations



Configurations 0-7

Experiment configurations



Configurations 8-16

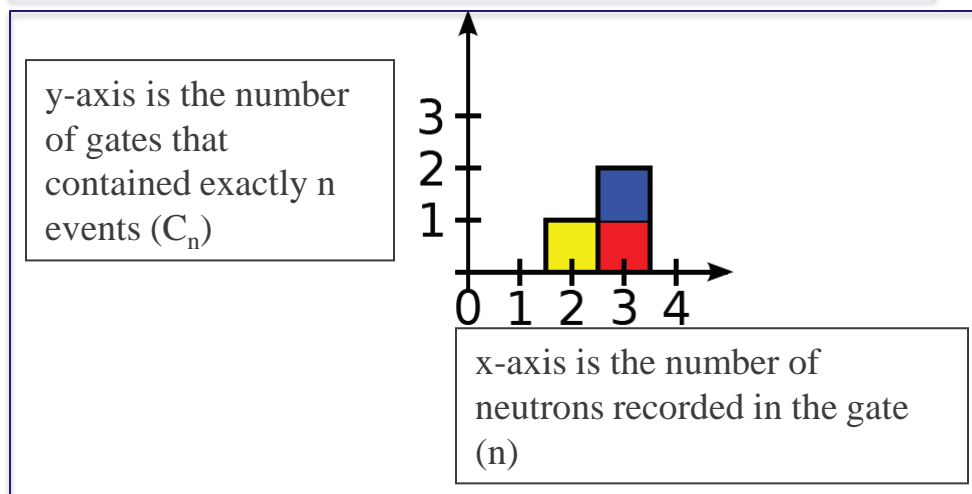
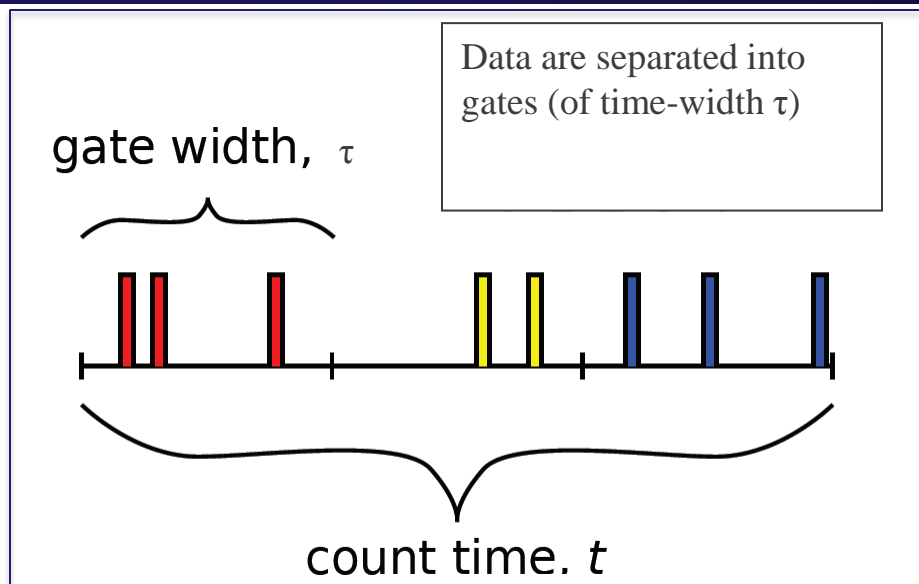
Preliminary Results (CED-3B + CED-4A)

Analysis method

- **Neutron noise analysis**

- Rossi-alpha
- Time interval analysis
- Feynman variance to mean
 - Hansen Dowdy
 - **Hage-Cifarelli**
- Others...

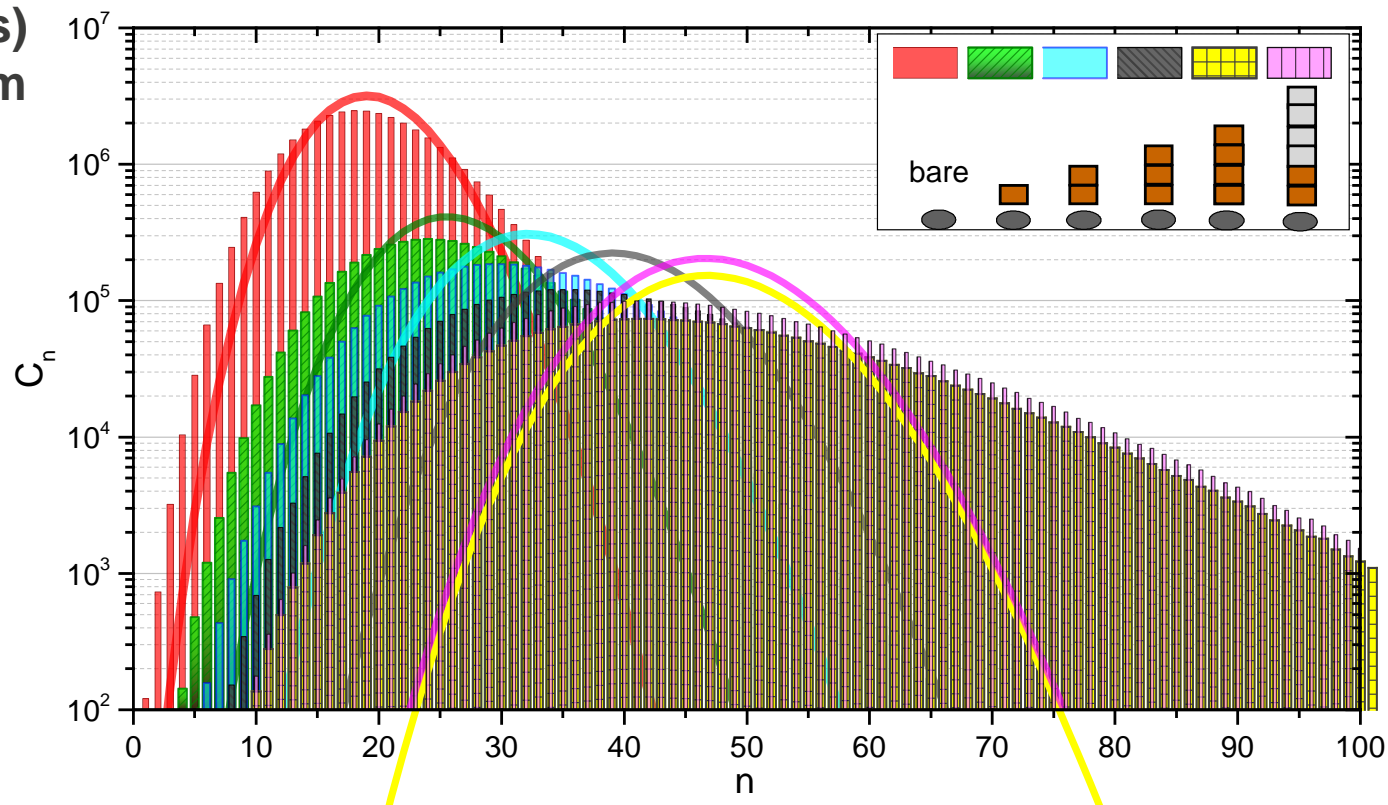
- **Analysis method used here is documented in detail in the BeRP/Ni and BeRP/W ICSBEP evaluations.**



Feynman histogram results

- Deviation from Poisson (solid lines) increases as system multiplication increases.
- Mean of histogram is proportional to the detector count rate.
- Width of histogram is proportional to the doubles count rate.

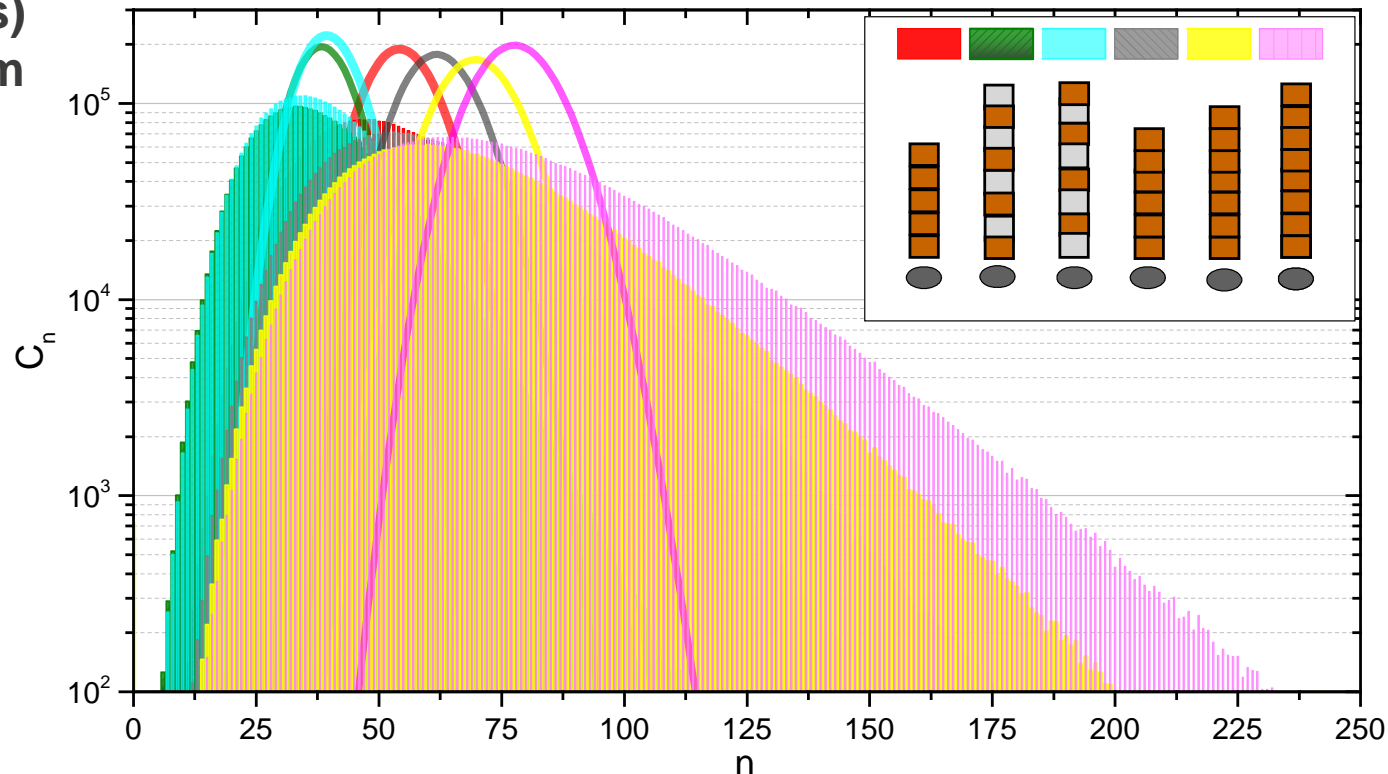
Configurations 0-5 (1024 micro-sec gate-width)



Feynman histogram results

- Deviation from Poisson (solid lines) increases as system multiplication increases.
- Mean of histogram is proportional to the detector count rate.
- Width of histogram is proportional to the doubles count rate.

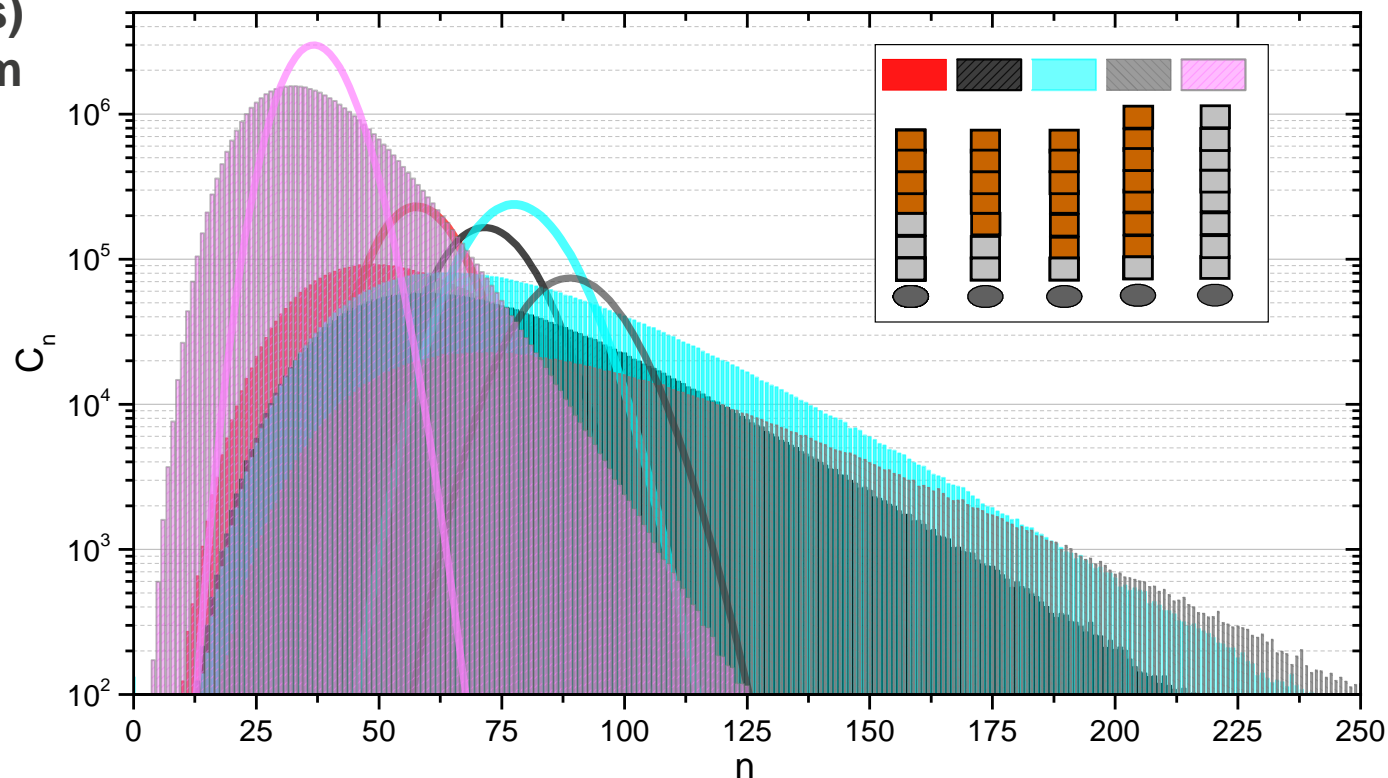
Configurations 6-11 (1024 micro-sec gate-width)



Feynman histogram results

- Deviation from Poisson (solid lines) increases as system multiplication increases.
- Mean of histogram is proportional to the detector count rate.
- Width of histogram is proportional to the doubles count rate.

Configurations 12-16 (1024 micro-sec gate-width)



Singles count rate (R_1)

Reduced factorial moment:

$$m_r(\tau) = \frac{\sum_{n=0}^{\infty} n(n-1)\cdots(n-r+1)p_n(\tau)}{r!}$$

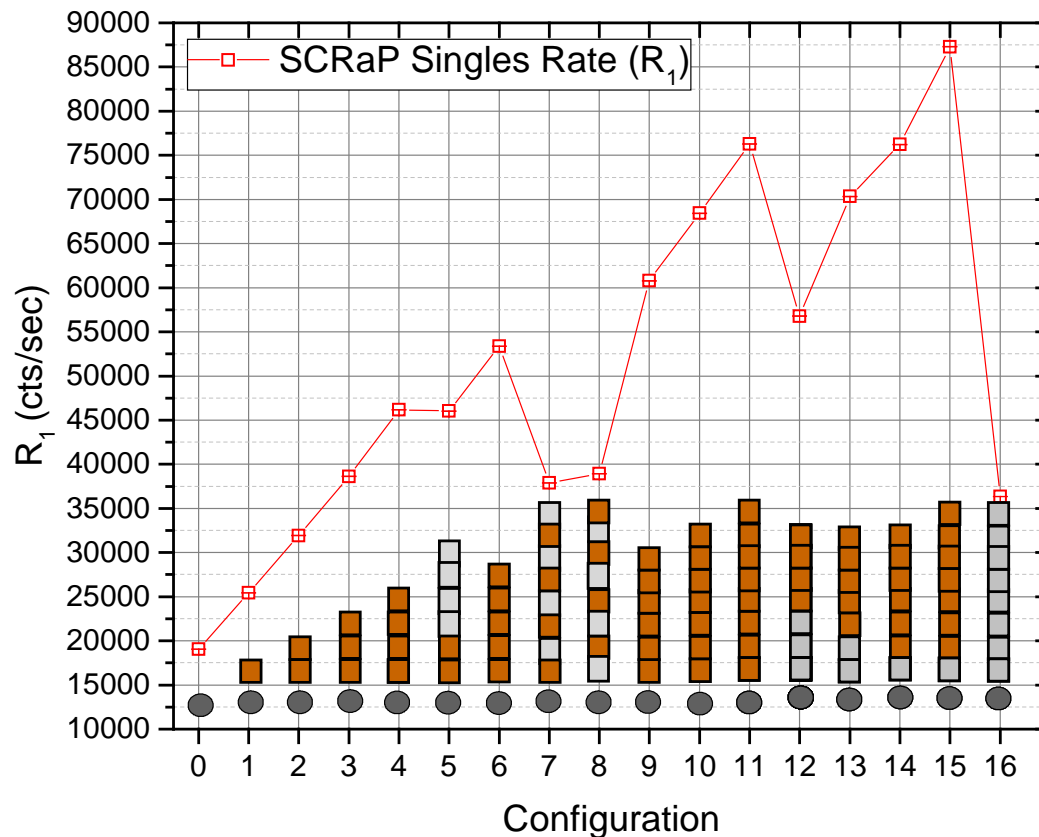
normalized fraction of gates that recorded n events:

$$p_n(\tau) = \frac{C_n(\tau)}{\sum_{n=0}^{\infty} C_n(\tau)}$$

Singles count rate:

$$R_1(\tau) = \frac{m_1(\tau)}{\tau}$$

Gate-width (τ)



Singles count rate (R_1)

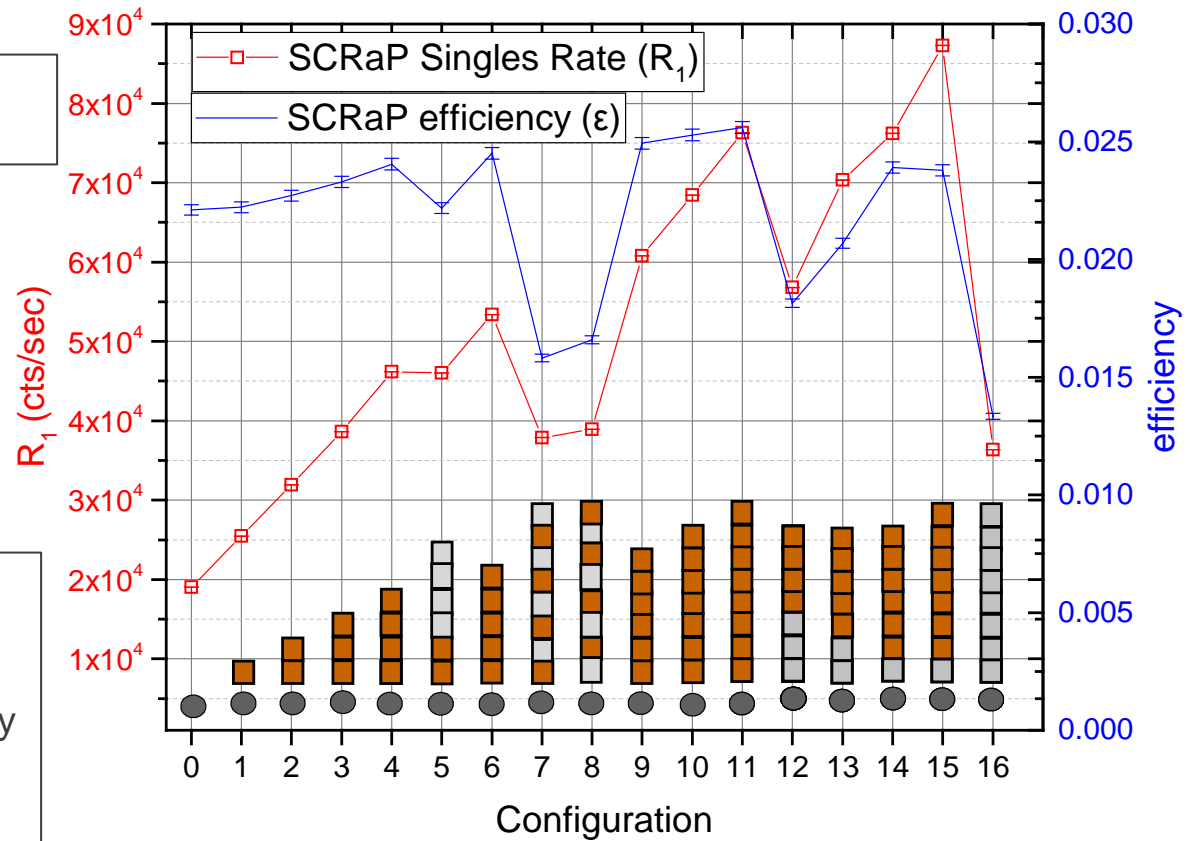
Detector efficiency (from Cf-252 measurements):

$$\epsilon = \frac{R_1(\tau)}{F_S \nu_{S(1)}}$$

This is the count rate from the Cf-252 measurements.

F_S is the reported spontaneous fission emission rate of the Cf-252 source.
 $\nu_{S(1)}$ is the average number of neutrons emitted per Cf-252 fission.

Plotted together to show that the reason that the count rate goes down significantly for the configurations with HDPE is due to the decrease in efficiency (which is caused by neutron absorption primarily in the hydrogen).

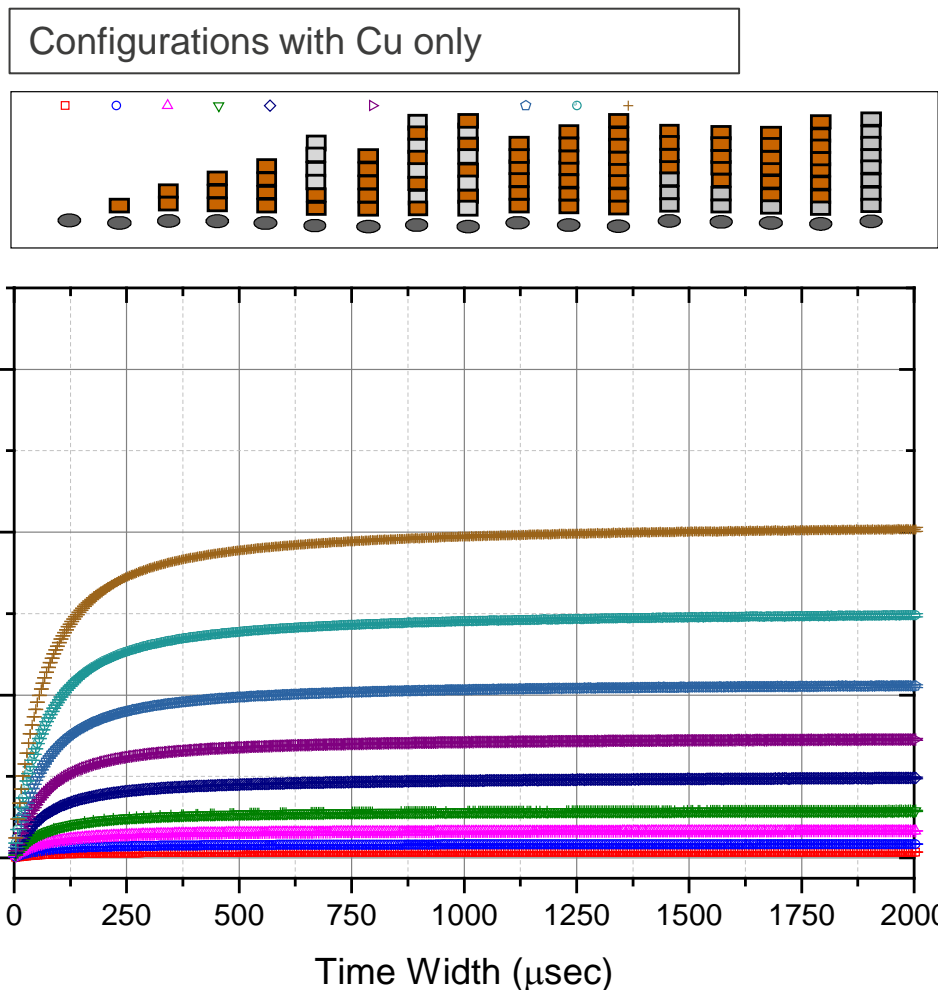


Excess variance

The excess variance (deviation of a Feynman histogram from a Poisson distribution) is proportional to Y_2 , given by:

$$Y_2(\tau) = \frac{m_2(\tau) - \frac{1}{2}[m_1(\tau)]^2}{\tau}$$

The amount of excess variance increases with Cu thickness (due to an increase in the system multiplication).



Excess variance

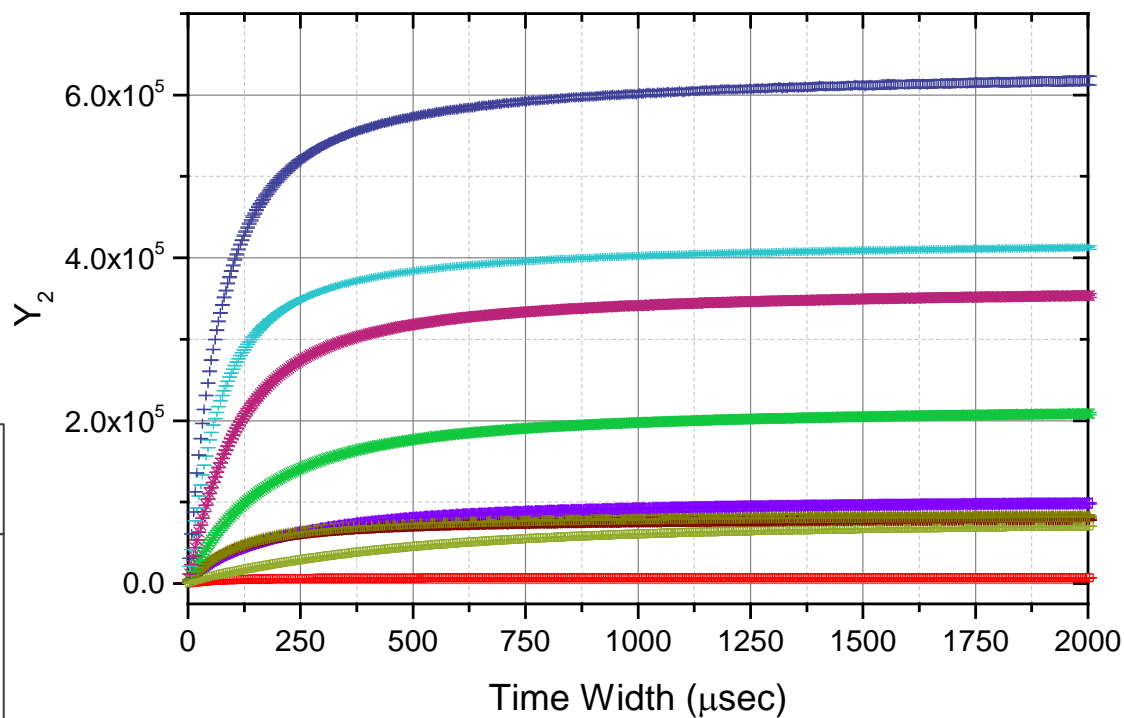
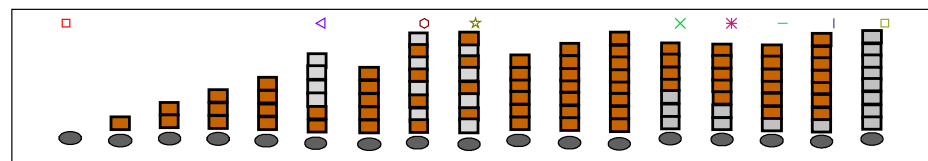
The excess variance (deviation of a Feynman histogram from a Poisson distribution) is proportional to Y_2 , given by:

$$Y_2(\tau) = \frac{m_2(\tau) - \frac{1}{2}[m_1(\tau)]^2}{\tau}$$

The amount of excess variance increases with the system multiplication.

HDPE can increase or decrease Y_2 (due to a competition between multiplication and detector efficiency (due to absorption in H)).

Configurations with Cu+HDPE



Neutron lifetime/slowing-down time

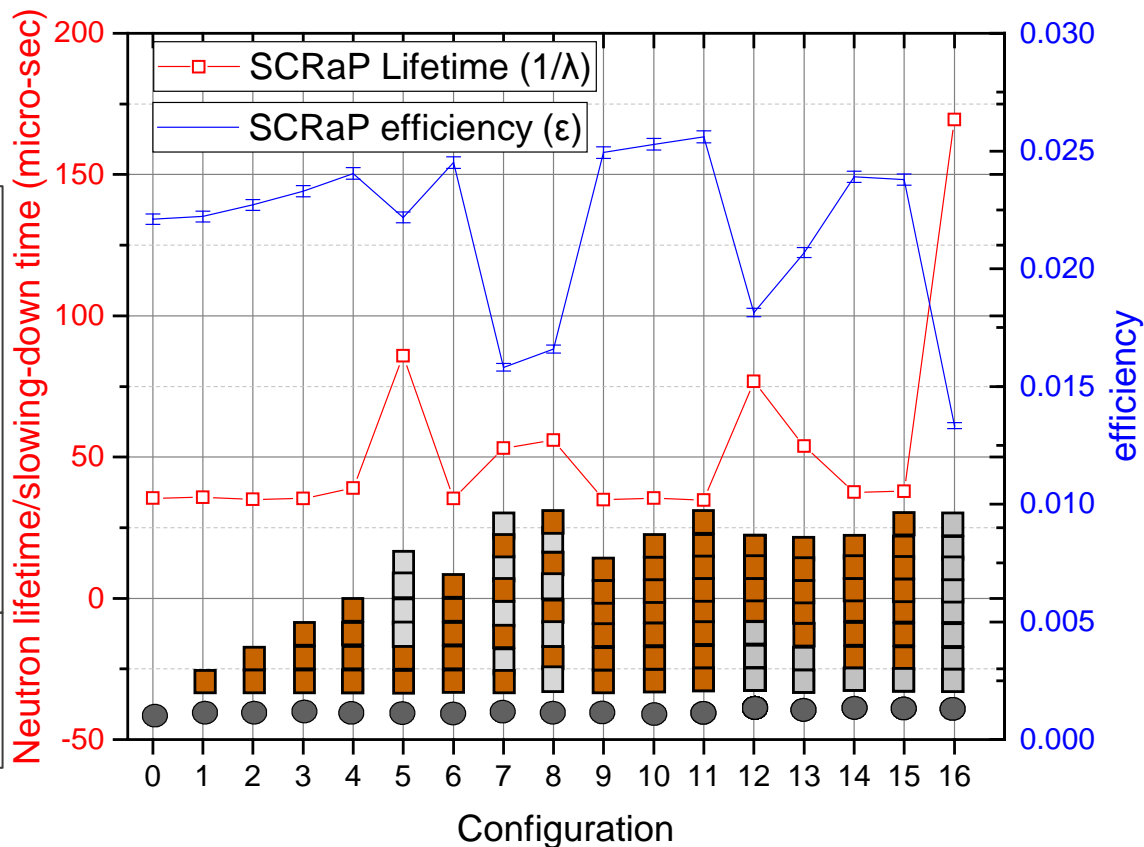
A fit can be performed on the Y_2 curves to calculate the neutron lifetime/slowing-down time ($1/\lambda$):

$$\omega_2(\lambda, \tau) = 1 - \frac{1 - e^{-\lambda\tau}}{\lambda\tau}$$

The MC-15 detector system has a slowing-down time of around 35 micro-seconds.

For the configurations with Cu only, the result is approximately 35 micro-seconds as expected, but it is significantly larger for the configurations that include HDPE hemishells.

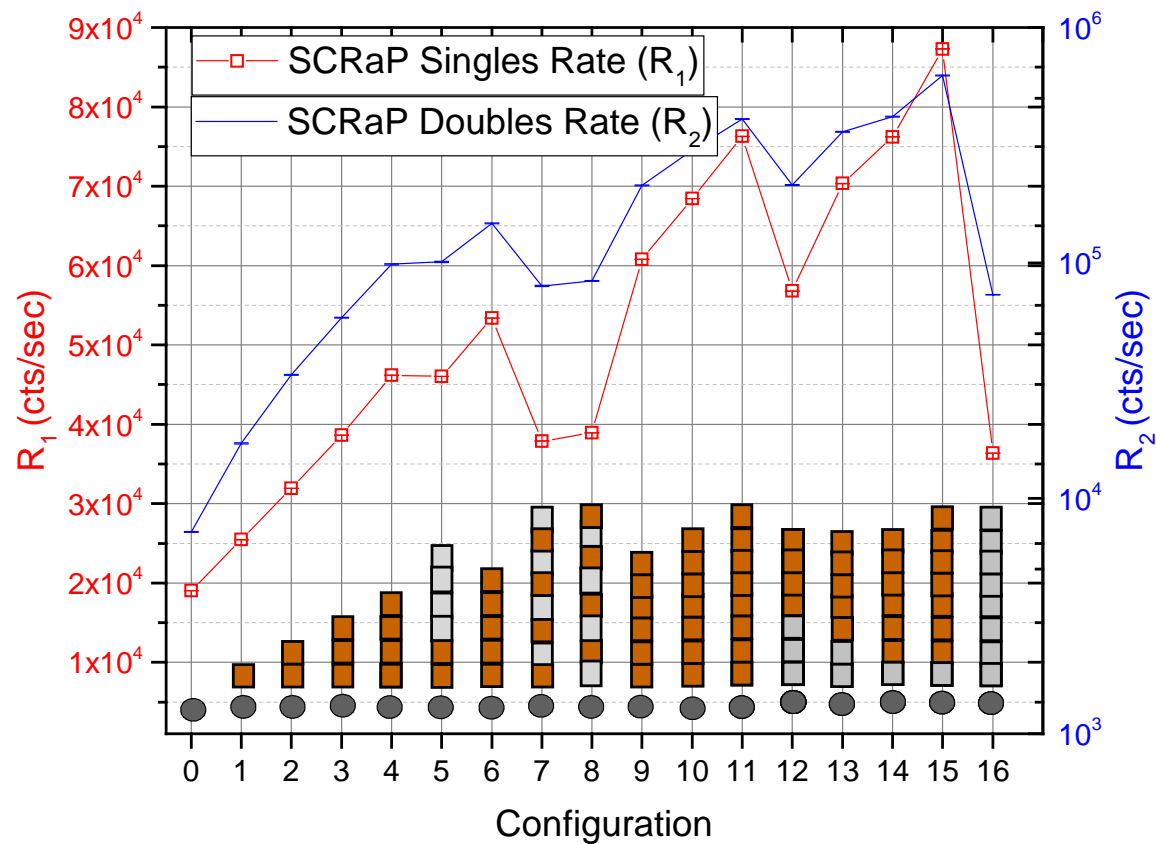
This can also be determined via Rossi-alpha analysis.



Doubles count rate (R_2)

Doubles count rate:

$$R_2(\tau) = \frac{Y_2(\tau)}{\omega_2(\lambda, \tau)}$$



Leakage multiplication (M_L)

$$M_L = \frac{-C_2 + C_4}{2C_1}$$

with

$$C_1 = \frac{\bar{\nu}_{S(1)} \bar{\nu}_{I(2)}}{\bar{\nu}_{I(1)} - 1}$$

$$C_2 = \bar{\nu}_{S(2)} - \frac{\bar{\nu}_{S(1)} \bar{\nu}_{I(2)}}{\bar{\nu}_{I(1)} - 1}$$

$$C_3 = -\frac{R_2(\tau) \bar{\nu}_{S(1)}}{R_1(\tau) \epsilon}$$

$$C_4 = \sqrt{C_2^2 - 4C_1 C_3}$$

$\bar{\nu}_{S(1)}$ 1st factorial moment of Pu-240 P_v

$\bar{\nu}_{S(2)}$ 2nd factorial moment of Pu-240 P_v

$\bar{\nu}_{I(1)}$ 1st factorial moment of Pu-239 P_v

$\bar{\nu}_{I(2)}$ 2nd factorial moment of Pu-239 P_v

Assumes that there are no emissions from (α, n) neutrons.

Leakage multiplication is related to the multiplication factor (k_{eff}).

Leakage multiplication (M_L)

$$M_L = \frac{-C_2 + C_4}{2C_1}$$

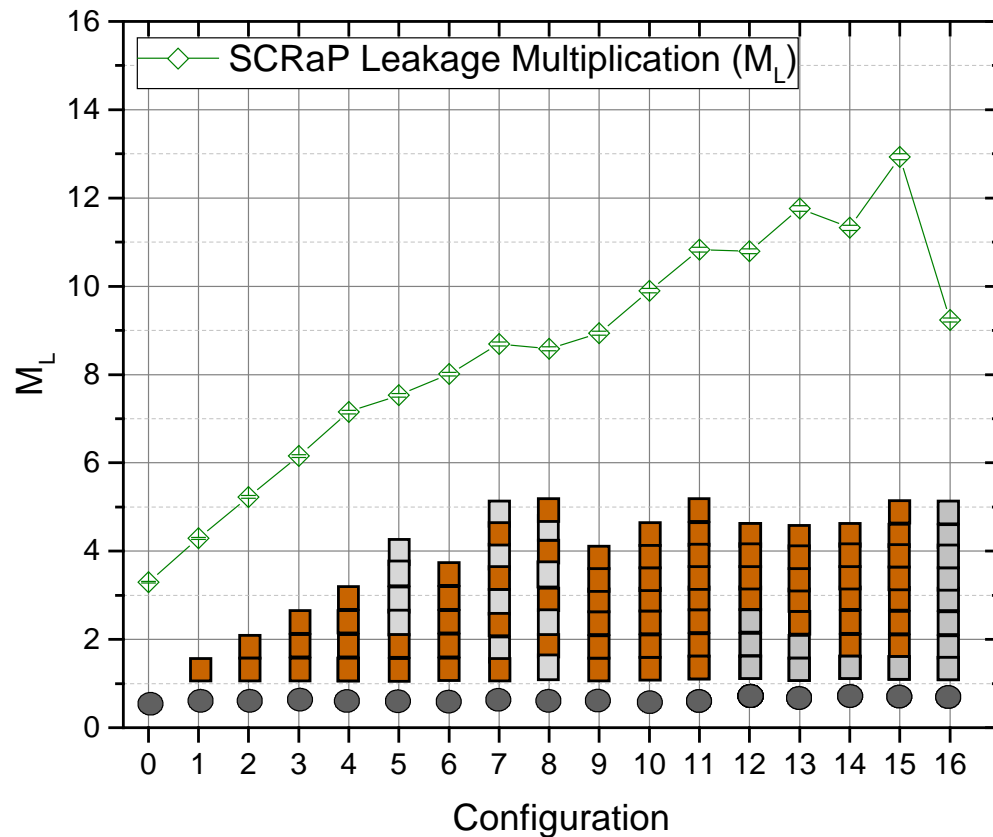
with

$$C_1 = \frac{\bar{v}_{S(1)} \bar{v}_{I(2)}}{\bar{v}_{I(1)} - 1}$$

$$C_2 = \bar{v}_{S(2)} - \frac{\bar{v}_{S(1)} \bar{v}_{I(2)}}{\bar{v}_{I(1)} - 1}$$

$$C_3 = -\frac{R_2(\tau) \bar{v}_{S(1)}}{R_1(\tau) \epsilon}$$

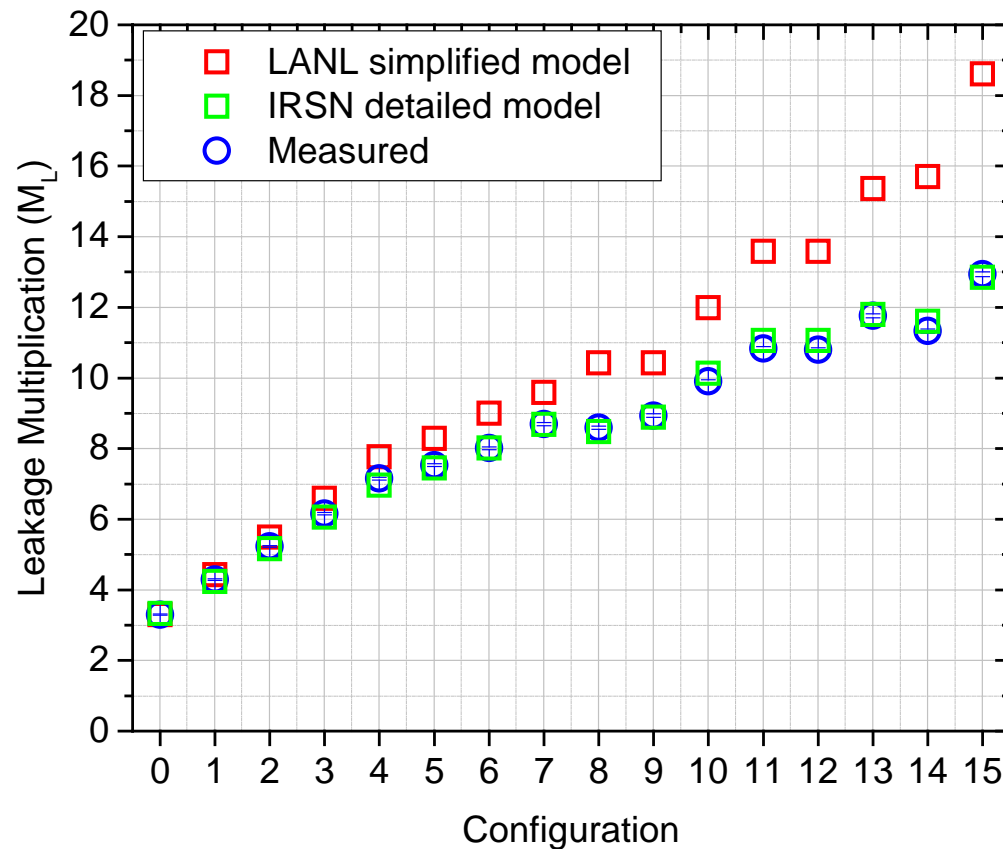
$$C_4 = \sqrt{C_2^2 - 4C_1 C_3}$$



Leakage multiplication (M_L)

As previously discussed, preliminary simulations provided multiplication factor (k_{eff}) results. These results were used to approximate leakage multiplication.

The LANL MCNP models were simplified models (perfect spherical reflectors with no materials present outside the reflectors) but the IRSN MORET models had additional details (MC-15 detectors, detailed reflector hemishells, etc.).

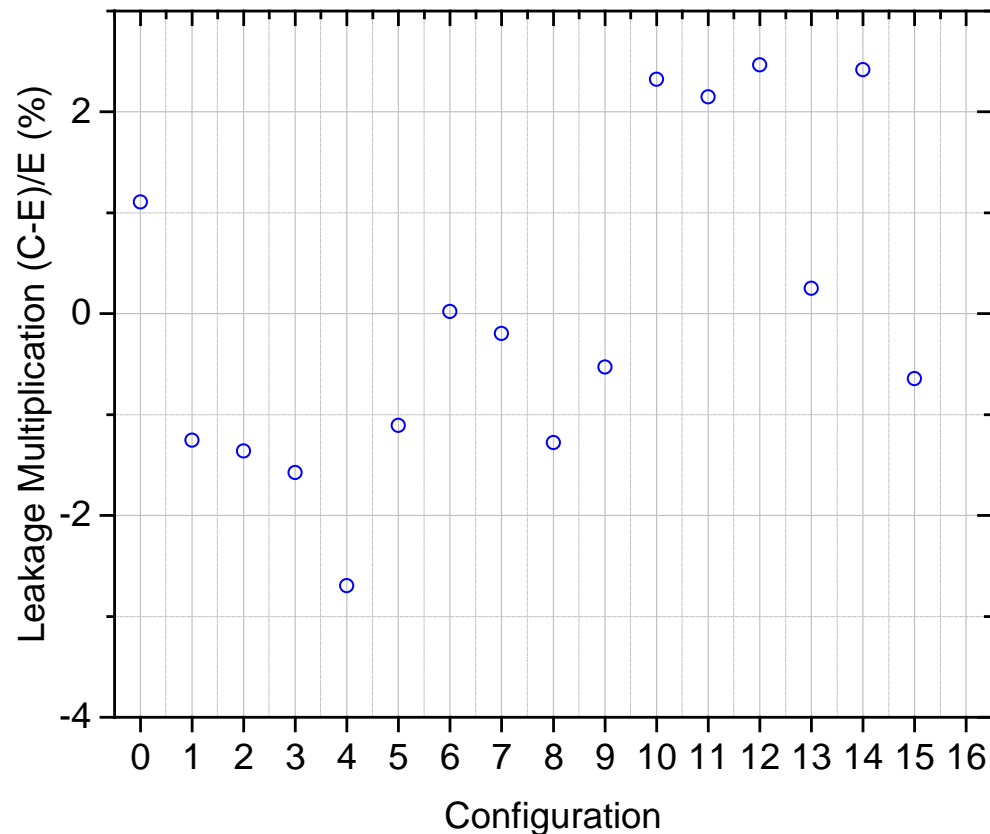


Leakage multiplication (M_L)

As previously discussed, preliminary simulations provided multiplication factor (k_{eff}) results. These results were used to approximate leakage multiplication.

The LANL MCNP models were simplified models (perfect spherical reflectors with no materials present outside the reflectors) but the IRSN MORET models had additional details (MC-15 detectors, detailed reflector hemishells, etc.).

(C-E)/E (%) for IRSN MORET detailed models



Future work (CED-4A + CED-4B)

What's next?

- This experiment will be evaluated and documented in an upcoming version of the ICSBEP handbook.
- Results will hopefully be used to improve cross-section libraries.
- Data set will also be used to validate subcritical analysis methods.



Thank you for your attention.



This work was supported by the DOE **Nuclear Criticality Safety Program**, funded and managed by the National Nuclear Security Administration for the Department of Energy.